nature reviews earth & environment

https://doi.org/10.1038/s43017-024-00587-1

Review article

Check for updates

The occurrence, mechanisms and hazards of large landslides along tablelands

Tomáš Pánek[1] ✉, Kristian Svennevig[2], Michal Břežný[1] & Piotr Migoń[3]

Abstract

The largest terrestrial coalescent landslide areas of the Earth, spanning hundreds to thousands of square kilometres, occur along the fringes of relatively low-relief sedimentary and volcanic tablelands. However, difficulties in landslide recognition in these areas have led to underestimations of their frequency and likelihood. In this Review, we explore the global distribution, controls and dynamics of landslides occurring along tableland fringes. Landslide fringes are caused by the uninterrupted and extensive presence of weak sub-caprock lithologies below a more competent caprock. Topography, escarpment height and caprock thickness do not affect landslide size but can locally influence the type of displacement. Rotational landslides dominate most landslide fringes and will eventually lead to tableland consumption over million-year timescales. Some tableland rims can generate catastrophic long-runout rock avalanches or earthflows, which might in turn trigger tsunamis, river avulsion or outburst floods. Tablelands can also fail by slow (centimetre per year) landslide movements sufficient to cause damage to infrastructure. These hazards are increasing especially in high-latitude tablelands owing to cryosphere degradation, as observed in Western Greenland. A more detailed global inventory of landslide fringe activity is urgently needed to better quantify these potential hazards.

Sections

Introduction

Distribution and characteristics of failed tablelands

Mechanisms of tableland failure

Factors influencing tableland instability

Landslide triggers

Tableland failure over geological time

Summary and future perspectives

[1]Department of Physical Geography and Geoecology, University of Ostrava, Ostrava, Czech Republic. [2]Geological Survey of Denmark and Greenland, GEUS, Copenhagen, Denmark. [3]Institute of Geography and Regional Development, University of Wrocław, Wrocław, Poland. ✉e-mail: tomas.panek@osu.cz

Key points

- Coalescent landslides found along tablelands in eastern Patagonia, the Colorado Plateau, the central Sahara, West Greenland and Central Asia cover areas spanning hundreds to thousands of square kilometres.
- Landslide fringes emerge from the coalescence of numerous individual landslides over time and space, occasionally in conjunction with larger catastrophic events.
- Giant tableland landslide fringes are influenced by geology, particularly weak rock occurrences at escarpment bases, with the lateral distribution of these units dictating the extent of landslide areas. Topography, escarpment height and caprock thickness do not affect landslide size but can locally influence the type of displacement.
- Retrogressive rotational landslides, prevalent along tableland fringes, were often assumed to be fossilized or inactive, especially in arid regions. Satellite monitoring reveals that some landslide rims, even in arid regions, show movements in the order of centimetres per year.
- Tableland fringes can also experience earthflows and catastrophic rock avalanches. Long-runout landslides can result in the damming of valley floors or landslide tsunamis, which can in turn trigger a chain of other hazards, such as flooding, river avulsions or outburst floods.
- Future research should aim to build a broader global inventory of failed tablelands, through increased interferometric synthetic aperture radar-based monitoring and more extensive radiometric dating of known landslides along tableland rims.

Introduction

Landslides, ranging from very slow (millimetre per year) to extremely rapid (metre per second) displacements[1] and involving volumes up to 10^{10} m^3 in subaerial settings[2], pose substantial natural hazards, particularly in mountain regions[2–4]. It is usually assumed that the largest documented subaerial landslides, as well as those most disastrous ones such as extremely rapid rock avalanches and rockslides, primarily occur in the highest mountains of the world[2,5]. However, some of the largest coalescent subaerial landslide areas documented on Earth affect the margins of relatively low-relief sedimentary and volcanic tablelands[6], rivalling or even exceeding the size of those found in alpine mountain ranges.

Tablelands comprise horizontal or gently dipping layered sedimentary[7] or volcanic rocks[6] that form extensive (thousands to tens of thousands of square kilometres) continental plateaus fringed by a steeper escarpment on at least one side. Horizontal competent caprocks (such as sandstone, limestone and volcanic rocks) form a strong or resistant layer that sits atop weaker sub-caprock materials (such as shales, clays and evaporites; Fig. 1a). The continuous exposure of weak rocks along tens to hundreds of kilometres of tableland rims makes them highly susceptible to landslides, leading to the formation of coalescing landslide fringes (Fig. 1b). These coalescing landslides typically create stepped hillslope topography, consisting of alternating steep segments (scarps) separated by benches and back-tilted surfaces (Fig. 1a). In eastern Patagonia, the Colorado Plateau, the central Sahara, West Greenland and Central Asia, coalescent landslide areas can cover hundreds to thousands of square kilometres. For example, in western Kazakhstan, landslides form a continuous 700-km-long rim on the western escarpment of the Ustyurt Plateau[8] and in eastern Patagonia, landslides affect more than 12,000 km^2 of volcanic mesas[6]. These landslide fringes create undrained depressions between landslide blocks, which in semiarid areas often become wetlands, attracting settlements, creating biological hotspots[9,10] and contributing to carbon storage[11].

However, previous assumptions have considered landslides along tableland fringes as non-catastrophic and slowly evolving over protracted timescales and have often been deemed ancient and stabilized[12–15]. Therefore, they have not received as much attention as landslides occurring in high mountain regions. Yet, some high tableland rims have generated catastrophic long-runout rock avalanches (such as the 2021 Assapaat frozen debris avalanche, Greenland, and the 2014 rock avalanche from Grand Mesa in the Colorado, USA)[16–18]. In addition, assumptions regarding the fossilized state of some landslide fringes were made before monitoring, and remote sensing observations revealed slow landslide movements in some tablelands on the order of millimetres to centimetres per year, which are sufficient to cause damage to infrastructure[19–22]. The observations of known failed tablelands are also biased towards arid regions, which are easily mapped through optical satellite imagery, and likely underestimate the number of tableland fringes in forested areas. As such, although there have been several global inventories focusing on giant catastrophic landslides affecting high mountains[2] and volcanoes[23], there has been no attempt so far to review large coalescent landslide areas affecting tablelands.

In this Review, we explore the distribution, mechanisms and triggers of landslides occurring along continental tablelands of the Earth. We examine landslides forming continuous fringes around volcanic or sedimentary tablelands (minimum length of 10 km) or single landslides in tablelands (area of at least 1 km^2). We exclude tablelands with numerous small, shallow, unconnected landslides and loess tablelands such as in China[24,25], as well as isostatically uplifted marine terraces with quick clay slides[26] as they do not fit our definition of tablelands characterized by layered rock formations with a caprock. Landslide fringes are also recognized in submarine settings[27–29] and beyond Earth, for instance, on Mars[30,31]. However, this Review focuses only on subaerial occurrences on Earth, although the mechanisms and morphology described might also apply elsewhere. Our objective is to evaluate landslide types, ages, activity and geological and topographical factors contributing to extensive coalescing landslide fringes, emphasizing climate change and cryosphere degradation impacts.

Distribution and characteristics of failed tablelands

The occurrence of large landslide fringes is limited by the distribution of the main sedimentary and volcanic tablelands (Fig. 2). Large landslide fringes have until now been detected on all continents except Australia. Although the areas of contiguous landslide fringes are seldom quantified in the literature, several published data sets indicate their enormous regional extent.

The most prominent clusters of large coalescent landslide areas with sizes exceeding 1,000 km^2 have been recognized in the Colorado Plateau[17,32,33], eastern Patagonia[6,34–37], Central West Greenland[38,39], central Sahara[12], the southern Sahelian zone of Niger[19,40], the Ogaden in Ethiopia[41] and the Ustyurt Plateau between the Caspian Sea and the Aral Lake[8,42] (Supplementary Table 1). Mapping in the volcanic

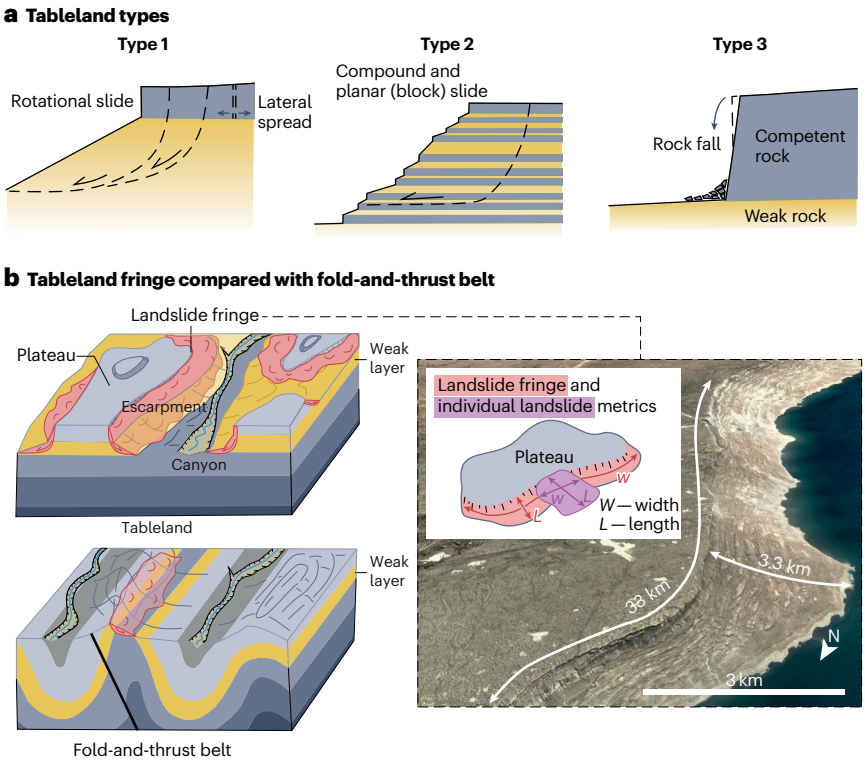

Fig. 1 | Tableland types and landslide fringes. a, Three types of tablelands. Type 1 tablelands have a hard layer of caprock (such as sandstones, limestone or basalt) with a steep escarpment, underlain by weaker sub-caprock layers (often shales, claystones or volcaniclastics), which slope more gently. This setup often results in deep-seated rotational slides along the tableland rim, occasionally dominated by lateral spreading. Type 2 tablelands have multiple layers of rocks with varied resistance that result in a stepped escarpment profile. Sliding planes are often located within thin intercalations of the weakest rocks, exhibiting planar or compound geometry. Type 3 tablelands have a uniform hard rock escarpment forming a simple steep cliff, which are primarily prone to local slope failures such as rock falls owing to the absence of soft layers exposed within the slope. **b**, The continuous exposure of weak rocks along tens to hundreds of kilometres of plateau rims makes tablelands highly susceptible to landslides, leading to the formation of frontal coalescing landslide fringes. For example, the landslide fringe along the eastern shore of Kara Bogaz Gol Bay in Turkmenistan extends for nearly 100 km; satellite image from Google Earth. By contrast, landslide-prone areas in fold-and-thrust belts are much narrower in extent (~1–10 km) owing to faulting and folding.

tableland of eastern Patagonia shows that the total area of landslides is ~30,000 km², with individual connected landslide complexes often exceeding 1,000 km². In the Ogaden sedimentary tableland, contiguous landslides cover an area exceeding 12,000 km² (refs. 41,43), whereas the rims of the Adar plateau in southern Niger are affected by landslides over an area of 10,000–15,000 km² (refs. 19,40). The western escarpment of the Ustyurt Plateau, east of the Caspian Sea, features a continuous landslide fringe spanning 1,200 km² (ref. 8), with some of the individual landslide bodies exceeding 200 km² (ref. 42). Although some of the largest rock avalanches in mountains and sector collapses of volcanoes rival the areas of landslide fringes in tablelands, most of these catastrophic landslides in those settings have areas at least an order of magnitude smaller[2].

The width of the landslide fringe (the length of landslide bodies between the head scarp and toe; Fig. 1) along escarpments is usually a few kilometres, but in the case of the Meseta del Lago Buenos Aires in Patagonia (Argentina) it is locally almost 12 km (ref. 34). In some coastal tablelands, such as the Nuussuaq Basin along the Vaigat Strait in West Greenland, the width of the landslide fringe is about 3–4 km, but locally, at the sites of long-runout rock avalanche deposits, it extends to more than 19 km and continues below sea level[38]. Some landslide fringes occur on entirely submerged escarpments, as observed offshore of Malta in the Mediterranean Sea[44]. They formed in subaerial conditions during the Last Glacial Maximum (LGM) ocean lowstand and were later inundated during the Holocene marine transgression[44,45]. In certain locations, such as the Ethiopian Highlands[46–49] and Iceland[50–55], failed tablelands lack long landslide fringes but feature individual large landslides covering several square kilometres[56,57].

Many classic tablelands, such as the Bohemian Cretaceous Basin[58–60], the Thuringia Basin in Germany[61,62], the Iberian Meseta in Spain[63,64], the Antrim Plateau in Northern Ireland[65,66] or those in southern Namibia[67], also contain numerous landslides, but these landslides are generally small (<1 km²), and the plateaus appear to lack continuous landslide fringes. However, in certain tablelands, such as the volcanic New England Tableland in eastern Australia[68], as well as in other temperate and tropical regions, the true extent of landslide fringes could be underestimated owing to challenges in identifying landslides in densely forested terrain.

In summary, failed tableland rims are among the largest subaerial landslide areas on the Earth. However, understanding their global distribution is still spatially biased, rather fragmentary, and requires further regional inventories.

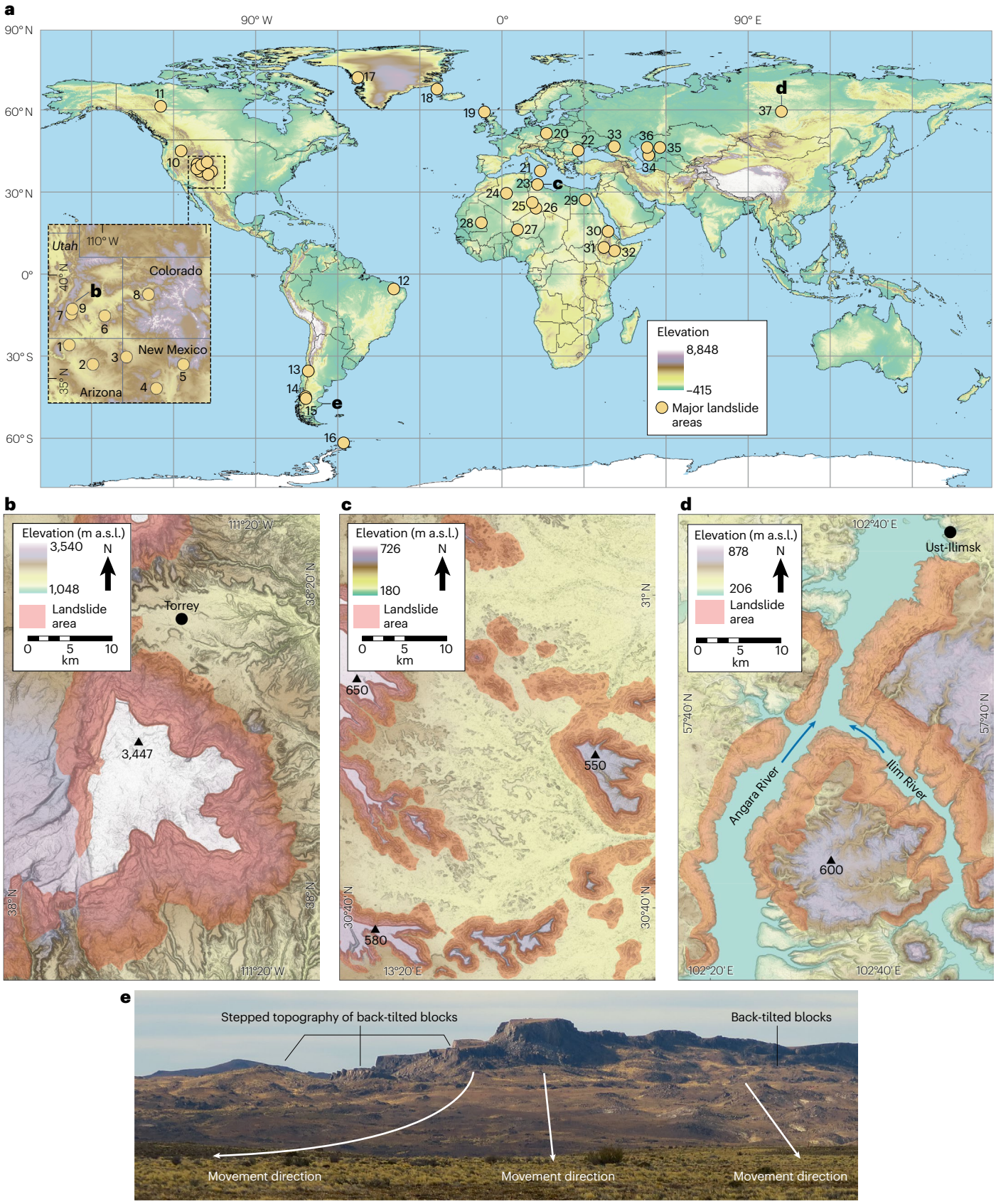
a
90° W
0°
90° E
90° N
60° N
30° N
0°
30° S
60° S
Utah
110° W
40° N
Colorado
New Mexico
Arizona
35° N
Elevation
8,848
−415
Major landslide areas
b
Elevation (m a.s.l.)
3,540
1,048
Landslide area
0 5 10 km
N
111°20′ W
38°20′ N
38° N
Torrey
3,447
c
Elevation (m a.s.l.)
726
180
Landslide area
0 5 10 km
N
31° N
30°40′ N
650
550
580
13°20′ E
d
Elevation (m a.s.l.)
878
206
Landslide area
0 5 10 km
N
102°40′ E
Ust-Ilimsk
57°40′ N
Angara River
Ilim River
600
102°20′ E
e
Stepped topography of back-tilted blocks
Back-tilted blocks
Movement direction
Movement direction
Movement direction

Fig. 2 | Global distribution and regional examples of failed tablelands. **a**, Distribution of major landslide fringes affecting tablelands, based on literature sources. The locations are numbered in accordance with Supplementary Table 1. **b**, Landslide fringe enclosing the high-elevated volcanic mesa of Boulder Mountain in the Aquarius Plateau in southern Utah, USA[96,97]. **c**, Isolated limestone plateaus, locally nearly consumed by landslides in the Saharan Hammada el Hamra, northern Libya[12,104]. **d**, Continuous landslide fringes flanking the Angara and Ilim Rivers incised into the basaltic traps in Siberia, Russia, just upstream of Ust-Ilimsk's water dam[127]. **e**, Example of fringed topography resulting from retrogressive rotational slides of the plateau edge, formed by Oligocene basalts overlying Cretaceous volcaniclastic rocks in the eastern Patagonian tableland (southwest of the town of Pico Truncado, Argentina). Although landslide fringes cover substantial areas along tableland margins, knowledge of their global distribution is geographically biased, especially towards regions with a long tradition of landslide research. a.s.l., above sea level.

Mechanisms of tableland failure

In tablelands, as in other settings, various landslide types can be expected with respect to kinematics and velocity[1]. However, certain types of landslides appear to be diagnostic for tablelands, mainly including rotational slides and spreads, with occasional but hazard-relevant long-runout earthflows and catastrophic rock avalanches.

Rotational slides and fringe complexity

Rotational slides[1] with deep-seated curved sliding surfaces, typically developing in mechanically weak rocks and soils[69], are the most common landslides forming continuous failed tableland fringes[6,8,12,17,32–34,70,71] (Fig. 1 and Supplementary Table 1). These slides, sometimes called slumps, create staircases of downthrown blocks tens to hundreds of metres high, with backslope tilt increasing towards the foot of the slope (Fig. 3a–c). Backslope tilt ranges from a few degrees to more than 60° (ref. 70). Such blocks, creating prominent landscape features at the escarpment base, are also referred to as toreva blocks, named after a location on the Black Mesa in northern Arizona[32]. The height of the blocks can range from tens to hundreds of metres. For instance, on the Grand Mesa in western Colorado[16,72] or along Chapada do Araripe in Brazil[71], the heights exceed 100 m. Along the eastern escarpment of Theban Plateau above the Nile River valley, blocks reach more than 200 m in height[70], and in the Scatter River valley in British Columbia, the sliding surfaces delineating the lower limit of blocks are situated at a depth of almost 300 m (ref. 73).

Although rotational sliding is typically the prevalent landslide mode in tablelands, block slides (planar slides[1]) with sliding surfaces entirely predisposed by slightly inclined bedding planes[22], or compound slides with both planar and rotational components of movement (Fig. 3d–f), predominate in certain areas (Fig. 1; ref. 73). Nevertheless, landslide areas flanking tableland rims are often even more complex, with slides being locally and/or temporarily replaced by toppling, lateral spreads (Fig. 3g), rockfall or earthflows[1], as documented on the Trotternish Peninsula in the northern Isle of Skye of Scotland[74].

Earthflows are particularly common on tableland marginal escarpments[37] and originate from weak sub-caprock layers with visco-plastic rheology[22,75] and/or fragmented landslide material, resulting from previous long-term rotational sliding[21,76]. Although they typically move slowly or in a pulse-like manner[1], this type of landslide can achieve a considerable runout, posing a hazard to infrastructure situated at a considerable distance from the scarp. Several earthflows, with lengths on the order of a few hundred of metres, have been activated since the beginning of the twenty-first century in the landslide fringe north of the city of Varna, Bulgaria, where slow movement continues, threatening local roads and buildings[77]. Earthflows, however, have the potential to achieve even greater runout distances. For instance, on the eastern slope of Chuska Mountain in New Mexico, an ancient 'mudflow' with runout more than 15 km (ref. 78) was described, extending well beyond an otherwise ~4–5 km wide landslide fringe. Accumulations of flow-like landslides forming the base of the landslide fringe on the northeastern margin of the Chapada do Araripe Plateau in Brazil exceed a length of 6 km (ref. 71). Several kilometre-long earthflows (referred to as mudflows by the authors in their original studies) have even been identified in the currently hyperarid environment of northeastern Niger[12,79].

Large-scale lateral spreads

Some tablelands are dominated by lateral spreading[80] (Fig. 3j–l and Supplementary Table 1), often leading to the complete disintegration of the entire tableland. In contrast to rotational landslides, movements within large-scale lateral spreads involve nearly horizontal movements of blocks, often accompanied by the sinking of caprock units into underlying weak strata and the opening of trenches and grabens. The largest rock spreads evolve across the entire plateaus. Examples of these extensive spreads, resembling the scale of extensional tectonics, have been documented in the Canyonlands on the Colorado Plateau[81,82] (Fig. 3k), the Ethiopian Ogaden[41] (Fig. 3j) and in the eastern Patagonia[6].

A common characteristic of these extensive spreading areas is that the sub-caprock units consist of evaporites containing minerals such as halite, carnallite and sylvite, making them susceptible to halokinesis and evolution of salt diapirs[41,81,82]. Lateral unloading owing to valley incision leads to salt flow, reflected in the deformation of the overlying caprock units through extension and the formation of horst-and-graben topography. In the Canyonlands, the depth of the graben reaches more than 100 m, with a length of several kilometres[81], making the area one of the most prominent gravity-induced landforms on Earth. Sliding planes in rock spreads create extensive décollements, which, in the Canyonlands, for instance, occur along the boundary between salt and gypsum[81,83]. Although only a few large-scale spreading provinces have been identified on Earth to date, their distribution is potentially greater, given the global extent of evaporites[84].

Catastrophic rock avalanches

Plateau rims can also be impacted by catastrophic rock avalanches (Fig. 2h,i and Supplementary Table 1), which are the most devastating and fatal types of mass movements[1,85,86]. Deposits of ancient rock avalanches have been described at the base of the Echo and Vermilion cliffs in Arizona[17] (Fig. 3i), in canyons incised into the Columbia River Plateau in Oregon[87,88], in Iceland[89] and in the Chapada do Araripe Plateau in Brazil, where a rock avalanche deposit covers an area of 10 km^2 and contains at least 100 million m^3 of material[71]. Several postglacial rock avalanches with a runout distance of up to 15 km have been documented originating from the Belgrano volcanic-sedimentary mesa in eastern Patagonia[36]. Extremely large marine-terminating tsunamigenic postglacial rock avalanches, with individual accumulation areas surpassing 100 km^2, a maximum runout of nearly 19 km and the largest accumulation volume exceeding 8 km^3, are located in West Greenland in the Vaigat Strait on a tableland formed by basaltic caprock overlying Cretaceous–Paleogene mudstones and sandstones[38] (Box 1).

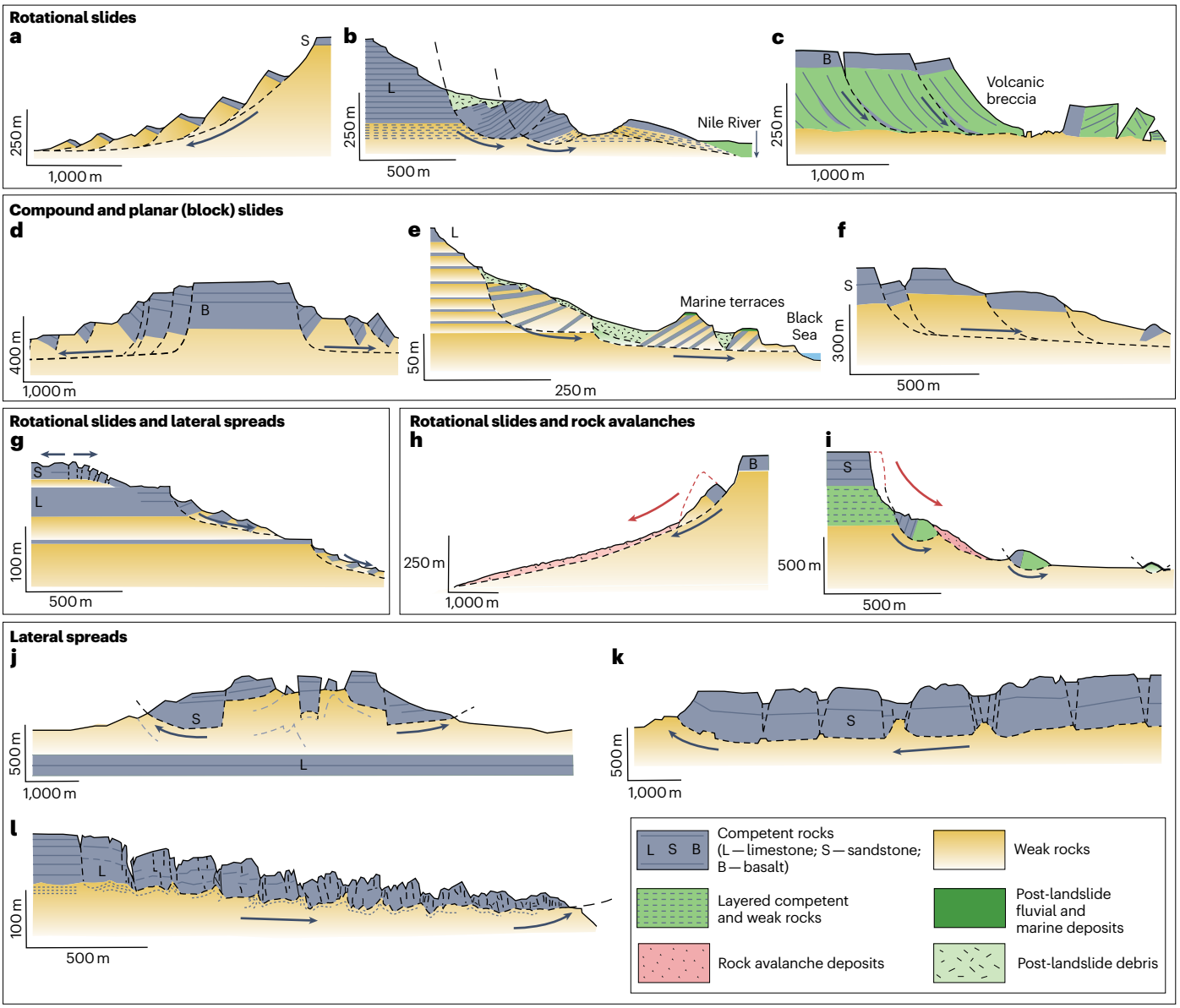

Fig. 3 | Landslide mechanisms occurring in failed tablelands. Note that geological cross-sections have different scales. **a**, Retrogressive rotational slide on the western escarpment of the Massak Mallat plateau, Niger[12]. **b**, Retrogressive rotational slide on the eastern edge of the Theban plateau, Egypt[161]. **c**, Retrogressive rotational slide along the eastern coast of the Ulu Peninsula, James Ross Island, Antarctica[135]. **d**, East–west cross-section of the whole Grand Mesa, CO, USA, showing retrogressive compound slides[72]. **e**, Compound slide on the Bulgarian coast of the Black Sea[21]. **f**, Compound slide with prominent planar (block) slide element in the upper part of the failed mass in the Scatter River valley, British Columbia, Canada[1]. **g**, Rotational slide combined with lateral spread (in the upper slope) in the Adar plateau in southern Niger[19]. **h**, Rotational slide which partly collapsed as rock avalanche in 2014 on the western slope of Grand Mesa, CO, USA[90]. **i**, Retrogressive rotational slide with an ancient rock avalanche on the Vermilion Cliff, AZ, USA[17]. **j**, Lateral spread affecting the whole plateau of Kebenawa Ridge in Ogaden, Ethiopia[41]. **k**, Lateral spread in Canyonlands, UT, USA[81]. **l**, Lateral spread partly accompanied by rotational slides in the Saharan Hammada al Hamra region, Libya[104]. In all cases, sliding surfaces are localized within weak beds, and catastrophic failures are preceded by slower processes such as rotational or compound slides and lateral spreads.

In 2014, an exceptionally large rock avalanche, sourced from rotational slides along the mesa rim, has been reported from the West Salt Creek Valley in the Colorado Plateau (Fig. 3h). The rock avalanche originated in May 2014 on the western slope of Mesa Grande, with a volume of 54.5 million m^3, making it one of the largest landslides in the US history[16]. The collapse, following an intense rain-on-snow event, occurred owing to the previous rotation and oversteepening of a large block formed by Eocene shales[16,90]. This case demonstrates that changes in slope geometry and the reduction of rock mass strength, resulting from long-term rotational movements, can eventually lead

to catastrophic collapse. However, some rock avalanches in tablelands could not have originated owing to preconditioning arising from previous long-term landslide activity, which altered topography and material properties along the fringe, but simply from in situ bedrock, for example, owing to the excessive height of the escarpment[71,91].

Although it is difficult to predict when, where and under what circumstances predominantly slow rotational slides and spreads in tablelands transform into long-runout earthflows or even catastrophic rock avalanches, the topography of the tableland rims and their lithological structure seem to be of particular importance.

Box 1 | Landslides and permafrost degradation in an Arctic tableland

Cryosphere degradation owing to climate change accelerates landslides in Arctic tablelands, with the most data available from Greenland. The Nuussuaq Basin is an up to 350 km long by 140 km wide geological basin exposed in Central West Greenland (see the figure, part **a**). It consists of Cretaceous–Paleogene clastic sediments capped by Paleogene volcanic rocks[162–164]. The Nuussuaq Basin holds 67% of all mapped landslides in Greenland; however, it represents only 4.7% of the ice-free area of Greenland[39]. The Vaigat Strait is located in the central part of the Nuussuaq Basin. Here, the clastic sediments of poorly consolidated sandstone and mudstone are exposed on slopes up to 900 m of elevation. The overlying caprock of hyaloclastite and basalt is up to 1,100 m thick. Nine, up to 8.4 km^3 volume, Early Holocene rock avalanches have been mapped here[38] and deposits from tsunamis triggered by some of these have been found in nearby lakes[132] (see the figure, the combined topography and bathymetry image, part **b**).

The Vaigat strait is also a hot spot for current landslides in Greenland as at least three of these, with volumes of up to 90 Mm^3, have occurred in 1952, 2000 and 2021 (refs. 18,137,138). The 1952 and the 2000 landslides caused destructive tsunamis. In 1952, one person died and structures were damaged in Qullissat. The 2000 Paatuut rock avalanche (see the figure, part **c**) caused damage to boats in Saqqaq. The 1952 and 2021 landslides were frozen debris avalanches sourced in massive talus deposits at the toe of the volcanic cliff forming the caprock of the tableland (see the figure, part **d**). The frozen debris avalanches were caused by progressive permafrost degradation and indicate that the hazards related to tableland failure in high latitudes could increase with ongoing climate change.

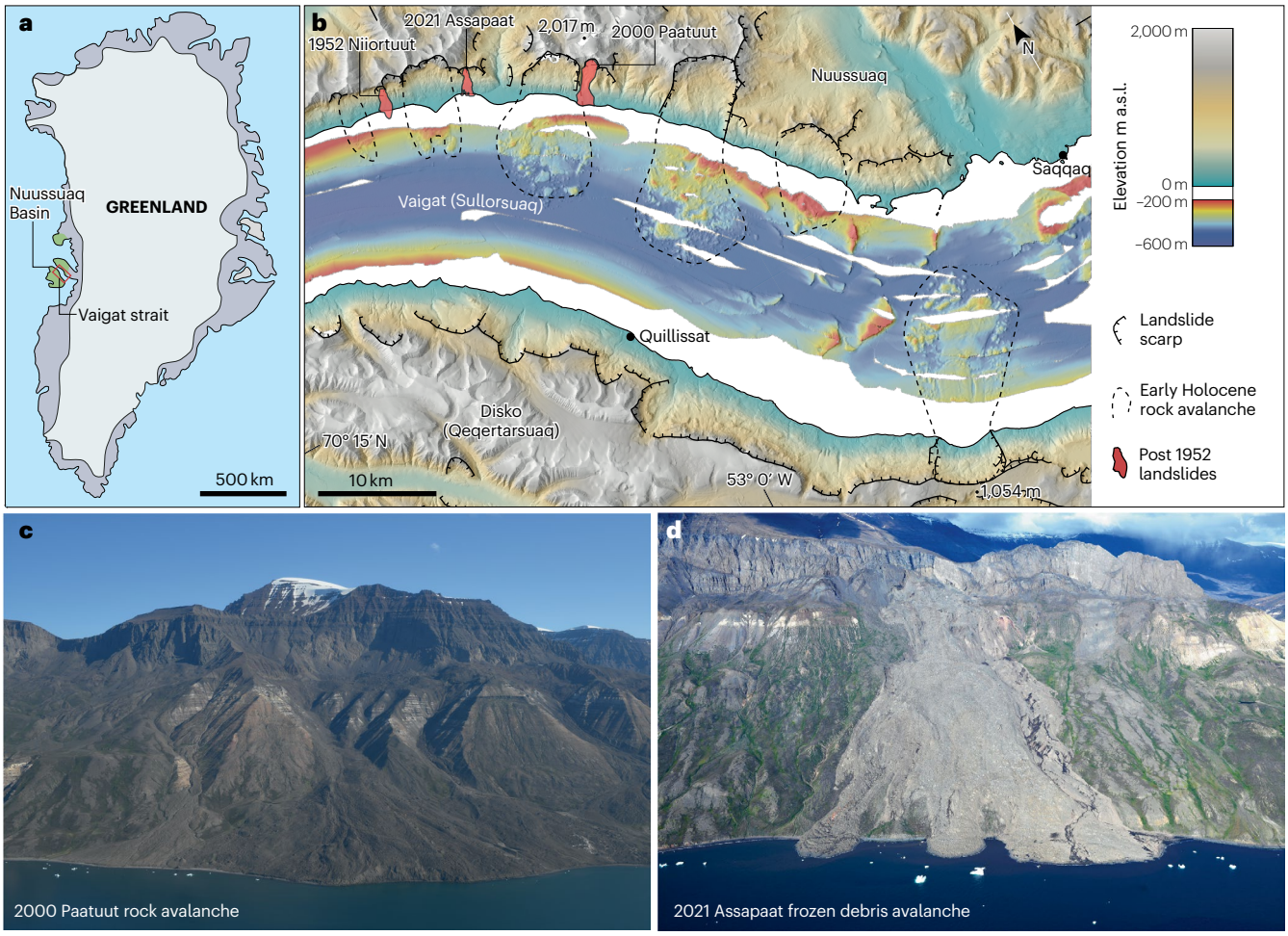

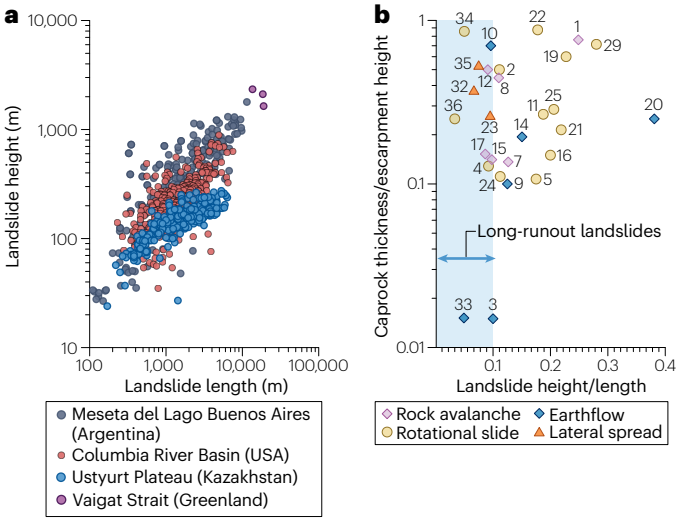

Fig. 4 | The relationships among landslide metrics, escarpment height and caprock thickness. a, Scatter plot depicting the length of landslides against escarpment height (approximated by the landslide elevation range) from the Patagonian tableland in Argentina (Meseta del Lago Buenos Aires)[34], Columbia River Basin in USA[87] and the Ustyurt Plateau in Kazakhstan[8]. The three largest rock avalanches from Vaigat strait (West Greenland)[38] are also included. The plot demonstrates comparable dimensions (length and height) of landslides across regions with contrasting escarpment heights. **b**, Scatter plot displaying the ratio of caprock thickness to escarpment height in selected locations of the largest landslide fringes of the world (site numbers are indicated in Supplementary Table 1). The landslide type represents the prevailing type at the surveyed site. There is no discernible influence of caprock thickness on landslide runout distance, even though the ratio varies considerably. Types of landslides: RS, rotational slide; RA, rock avalanche; EF, earthflow; LS, lateral spread.

Factors influencing tableland instability

Landslide predisposing factors make certain localities and settings more prone to slope instability. Although there are many potential predispositions, the combination of topographic and geological factors likely has a dominant role in the occurrence of extensive coalescent landslide fringes[17,34,87]. The largest landslides reported from high mountains are often on active tectonic plate boundaries[2]. By contrast, extensive landslide-affected tableland fringes mostly occur within stable continental platforms, with influences from active tectonics or seismicity observed only in specific cases, particularly in tablelands located near tectonically mobile orogens[36,92,93] or those experiencing enhanced seismic activity after deglaciation owing to glacial isostatic adjustment[51–57]. In addition, the edges of tableland landslide fringes often have relatively unrestricted development compared with landslides occurring in high mountain ranges, as the scale of ridges and valleys in high mountains partly dictates the size of landslides, as their development can be constrained by the limited width of valleys. Although topographic metrics and detailed information on the properties of rocks forming landslide fringes are still fragmentary (Supplementary Table 1), it is possible to infer at least the main factors controlling the extent and dimension of landslides in tablelands from the published literature, which we review in this section.

Topography of escarpments

The height, slope and length of escarpments determine the maximum potential extent of coalescent landslide fringes (Fig. 1). The heights of tableland escarpments typically range from tens of metres to more than 1 km (ref. 94). Landslide fringes can be found both on only 50–100 m high escarpments on the NW coast of Malta island[22,95] and on escarpments of more than 1,000 m in height in the Colorado Plateau region[96,97] or eastern Patagonia[34,36]. Similarly, local relief and valley depth were found to not affect the localization and clustering of landslides in Icelandic fjords[51,52,54,55]. Furthermore, local relief does not have a major impact on the dimensions of landslides; some of the largest landslides of the world around the tablelands east of the Caspian Sea in Kazakhstan occupy an escarpment ~100–200 m high and reach lengths of more than 5 km (Fig. 4a; ref. 8). In some cases, the movement of the landslide blocks occurred on very gentle slopes, with an inclination less than 5° (refs. 8,12,19).

Topographic metrics from landslides in the Meseta del Lago Buenos Aires in Patagonia[34], the Columbia River Plateau in Oregon[87] and the Ustyurt Plateau in Kazakhstan[8] show a general correlation between the height of mesa rim (approximated by the difference between the highest and lowest landslide points) and landslide length (Fig. 4a). However, inter-regional comparisons reveal that the dimensions of landslides are similar between regions with contrasting escarpment heights. Long landslides in the Columbia River Plateau require less escarpment height than those in the Meseta del Lago Buenos Aires, and substantially less height is needed in the Ustyurt Plateau compared with other tablelands (Fig. 4a). As such, under certain conditions, even relatively low escarpments can generate long-runout landslides. In the case of the western escarpment of the Ustyurt Plateau, landslides probably collapsed into the Caspian Sea during Late Quaternary transgressions[98] and were at least partially transported underwater, which increased their mobility[8].

To summarize, the height of the escarpment does not seem to affect the distribution of landslides in failed tablelands.

Escarpment stratigraphy and lithology

Surprisingly, some of the highest escarpments of the Earth lack major landslides, which appear to be rare in the high plateaus formed by very thick, competent sedimentary rocks, such as quartzites and sandstones that make up the Tepuis in Venezuela and Brazil[99]. Similarly, large coalescent landslides are absent in areas with thick continental flood basalts, such as the Paraná[100], Etendeka[67], Deccan Traps[101] and the Blosseville Coast in East Greenland. Likewise, only a few rather isolated landslides have been documented in the Karoo Supergroup volcanic and sedimentary rocks that form prominent escarpments in South Africa[102]. These examples suggest that geological structures have a major role in the predisposition of landslide fringes and merit further detailed evaluation.

Faults, joint systems and intrusions can locally predispose landslides in tablelands[36,92,93,103], but the horizontal or gently dipping stratification of rocks is a crucial precondition for the widespread occurrence of landslides in tablelands. This preconditioning is particularly evident in which mechanically weak rocks are exposed in continuous outcrops hundreds of kilometres long along the escarpments (Fig. 1). The key question is which properties of rocks and their stratification are crucial for landslide development. Traditionally, slope instability in tablelands has been attributed to rheological and hydrogeological contrasts between the caprock (such as sandstones, limestones and basalts) and underlying weak layers (such as shales, clays, claystones, marls, evaporites, volcaniclastics and poorly lithified sandstones). Landslides on Colorado Plateau escarpments occur exclusively when thick sandstones overlay thick shales, and escarpments composed solely of

competent or thin sandstones that limit groundwater accumulation do not experience landslides[14].

However, data from tablelands worldwide indicate that the thickness of caprock relative to the sub-caprock units might have a marginal influence on slope stability (Supplementary Table 1). The ratio between caprock thickness and escarpment height does not impact the occurrence, dimensions and types of landslides on tableland rims either (Fig. 4b). In some tablelands, long-runout landslides originate both from escarpments, in which the caprock represents more than half of the height of escarpment[17,42,87], and from those where it constitutes only about one-tenth of the height of escarpment (Fig. 4b; refs. 8,16,38). Caprock thickness can vary considerably within a single landslide area without reflection in landslide metrics or kinematics. Likewise, there appears no relationship between landslide type and the share of caprock in the total escarpment height. Caprock can constitute either the majority or a negligible fraction of the stratigraphical sequence exposed in the escarpment, and still both catastrophic (such as rock avalanches) and slow-moving (rotational slides) endmembers of a landslide spectrum in tablelands are reported from these escarpments (Fig. 4b).

In contrast to the properties of caprock, the properties of sub-caprock lithologies are more important to the stability of tableland rims. The shear strength of sub-caprock units appears crucial for landslide development because landslides are initiated and sliding surfaces are formed within the weakest beds outcropping within the escarpments[17,20,21,33,104,105]. The dip of these weak beds relative to the orientation of the escarpment usually has no influence. Although some landslides in tablelands are predisposed by a slight out-of-slope dip of strata and originate as planar or compound slides[17,33,42,73], in most cases, the sliding surfaces are not governed by the dip of lithological contacts. On some plateaus, an equally wide landslide rim is found on slopes built by layers gently dipping towards the massif and on the opposite slopes, where the strata dip gently outward[17,72].

Sliding surfaces are typically found in the weakest rocks present within sub-caprock units, often exhibiting specific lithological properties. These are usually smectite-rich claystones[12,104,106], evaporites such as gypsum or salt[12,42,81], overconsolidated claystones and shales[17,107], or liquefiable sands[78]. The lateral continuity of such strata contributes to the substantial length of landslide fringes. For example, shales of Triassic Chinle Formation form the base of escarpments over a large area of the Colorado Plateau and predispose landslide fringes hundreds of kilometres long around the plateau[17,108]. Within the nearly 1,000 m thick sedimentary rock sequence of the Grand Canyon in the Surprise Valley area, the presence of an ~45 m thick shale layer within the Cambrian Bright Angel Formation was indispensable for the formation of sliding planes in all landslides[33].

In these weak layers, however, it is often only metre-scale intercalations with substantially reduced shear strength that are crucial for slope instability. For example, many landslides on the Colorado Plateau are initiated in layers formed by weathered volcanic ash, which are only a few metres thick and intercalated within the shales of the Petrified Forest Member of the Triassic Chinle Formation[17]. In this case, the ash beds have a cohesion of 4.8 kPa and a friction angle of 11° — just more than 2% cohesion and one-fifth the friction angle of the Jurassic Navajo Sandstone forming the caprock. Although the cohesion of these intercalations is similar to the surrounding Petrified Forest Member, the friction angle contributes only about one-third of the strength of these shales[17]. In other words, particularly low values of one of the geomechanical characteristics (in this case, the friction angle) within thin intercalated beds can be crucial for the occurrence of a landslide in layers that are already very weak. These geomechanical characteristics imply that a high-resolution understanding of the lithostratigraphy and geotechnical properties of individual layers within complex sedimentary formations is often necessary to assess the stability and susceptibility of tablelands to be affected by large landslides. Furthermore, the strength of soft rocks tends to rapidly decrease during landslide development, for example, claystones transform into plastic clays through remoulding[72] and weaken during shearing owing to dilation, rearrangement of clay minerals and increase in water-holding capacity[107]. These processes involve stresses during landslide movement that disturb the rock structure.

More complicated stratigraphy of an escarpment, characterized by more frequent alternations of competent and weak beds, could also constrain the development of landslides. As a result, a landslide might exhibit a step-like pattern, with several unconnected landslide levels separated by benches predisposed by more resistant layers (Fig. 3g; refs. 19,40,103). A stiff layer at the base of the escarpment can have a critical impact on reducing the strength of overlying weak beds where a sliding plane is formed[17]. Above the rigid layer, the concentration of deformation in the soft material increases plasticity, facilitating the development of a sliding surface upon the removal of lateral support (for example, due to erosion).

Differences in rock permeability can also have a substantial role in the formation of landslides. Hard and jointed caprock often has higher permeability than the sub-caprock, which can act as an aquitard. Thus, water infiltrating through caprock is obstructed by sub-caprock, resulting in higher pore pressures, lubrication of potential sliding surfaces and reduced cohesion[17]. For horizontally or only very gently inclined layers, differences in caprock thickness might not have a role in water infiltration and related landslide predisposition (as previously hypothesized for isoclinally folded ridges[109]). In the case of tablelands, water can infiltrate simply through joints downwards to the sub-caprock. However, in the inclined beds, the preferential route might be in the dip direction of bedding planes[110] and water does not have to reach the sub-caprock in the areas with thick caprock[109].

We summarize that although the presence of weak beds is critical to the occurrence of landslides in tablelands, even subtle changes in local topography and how these topographic conditions combine with the overall geology often have a role in the development of different types of landslides, whether catastrophic or not. However, it is also crucial to consider the external factors that the tableland is exposed to during its geomorphological evolution and the triggers that act on slope stability.

Landslide triggers

The large coalescent landslide areas around the tablelands raise questions about their origins and triggers. Understanding the conditions under which they were active is crucial for assessing current hazards. Specifically, it is important to determine the potential for accelerated movements or catastrophic failures under today's conditions.

Climate triggers

Movements detected in a few monitored landslide fringes are typically very slow to slow, ranging from millimetres to centimetres per year[22,72,111]. However, many large landslides around tablelands have been presumed as ancient features that occurred during different climatic conditions, often during the wetter (pluvial) periods of the Pleistocene (Supplementary Table 1). This perspective is particularly prevalent in the current arid and semi-arid regions[12,32,78,112,113]. For example, landslides

in the Sahara, including those at Hamada al Hamra, Massak Mallat, Djado Plateau and Plateau du Mangueni, were thought to have occurred during a single major landslide phase in a wetter climate at the transition from the Pliocene to the Early Pleistocene[12]. Mudflows in northeastern Niger were also thought to have formed under conditions humid enough to allow the saturation and swelling of montmorillonite-rich clays[12], which constitute the primary predisposition of the landslides and, under dry conditions, form a very stiff material.

On the Colorado Plateau and in other regions of the American Southwest, landslides were traditionally associated with pluvial periods coinciding with the cold phases of the Pleistocene[14,108]. However, in other regions such as the Sahara and the Middle East, current knowledge suggests that pluvial periods coincide with the insolation maxima of interglacials or interstadials[114,115], potentially making the Holocene, especially during its climatic optimum, conducive to landslide formation. Although landslides in the Sahara are not directly radiometrically dated, there have been at least four humid phases in the past 160 ka[116,117] (the last one in the first half of the Holocene) when large river systems were activated across the Sahara. If rainfall was sufficient to feed large rivers, landslide fringes in the tablelands of the central Sahara can also be expected to have formed or been reactivated during these periods.

Chronological studies of failed tablelands are limited[15,33,36,37,95,113,118–120], and even when available, they might not reliably represent the age of entire landslide fringes that can extend for hundreds of kilometres along tableland rims. Nonetheless, absolute dating of some landslides suggests that they are at least of Late Pleistocene age[15,95] or predate the LGM[34]. For instance, the lower part of the landslide fringe on the Trotternish Peninsula on the Isle of Skye in Scotland was abraded by an ice sheet during its last advance[121], whereas the upper rotated blocks are postglacial and were detached from the headscarp before ~6.5 ka (ref. 118). Landslide blocks along the Grand Mesa in Colorado show glacial striations, suggesting a pre-LGM onset of landslide activity[16,72].

However, some evidence suggests that certain landslide fringes have a much longer geological history. The first cosmogenic exposure data from landslides in the Grand Canyon indicate that some landslide deposits are over two million years old[33]. Some landslides in eastern Patagonia appear to be even older. South of Lago Cardiel in Argentina, a 6 km wide landslide rim is overlain by a lava flow assumed to be of Lower Pliocene age (approximately 5 million years old)[122,123]; hence, the landslide must be older. Likewise, an older generation of rotated blocks at the eastern foot of the Theban Plateau near Luxor, Egypt, is covered by a Lower Pleistocene fluvial formation, indicating that the landslide area began to form in the Pliocene, whereas younger generations of landslides occurred during middle-late Pleistocene humid periods[124].

Although it is generally assumed that landslide fringes in arid areas are ancient and inactive, ongoing monitoring indicates that this inactivity might not always be the case. Applications of Earth observation monitoring facilities, especially interferometric synthetic aperture radar technology, show that at least some giant landslide areas in arid regions are moving in the order of centimetres per year[42]. On the western escarpment of the Ustyurt Plateau in Kazakhstan, some kilometre-scale landslides originated at least during the Late Holocene, although the main body of landslides dates back to the Pleistocene[8]. At Echo Cliffs, Arizona, a landslide over 350 m wide was reactivated in 2013 (ref. 125). This event, notable for hosting a landslide fringe deemed ancient and inactive in current conditions[17], lacked an evident meteorological cause. Instead, its occurrence is interpreted to be the result of long-term creep and strength degradation of plastic clays[125]. Even on some landslides in the central Sahara, where rainfall is less than 50 mm per year, the development of fractures indicating slow movements and disintegration of tableland margins has been observed[104]. These cases suggest that landslide fringes in certain arid regions are not necessarily relics of different climatic conditions.

Triggers from geological crises and compound hazards

Some large landslide areas can represent short-term 'geological crises'[126] — transitional periods in the landscape history of certain regions when one major or a combination of multiple external factors occurred, leading to widespread slope instability. For example, rotational slides combined with lateral spreads and earthflows along the western escarpment of the Ustyurt Plateau in Kazakhstan originated during the massive transgression (transgressions) of the Caspian Sea in the Late Pleistocene[8]. Landslides along the Vermilion and Echo Cliffs on the Colorado Plateau could have been triggered by the formation of lava-dammed lakes, elevating groundwater levels and causing saturation, thus reducing cohesion in the weak Chinle Formation; an alternative explanation suggests initiation by rapid drawdown following the failure of lava dams[17]. Giant landslides affecting basalt-capped plateaus along the banks of the Angara River in Siberia[127] might have been triggered by repeated catastrophic outflows caused by megatsunamis from Lake Baikal during the Pleistocene[128]. Last but not the least, the Messinian crisis ~5–6 Ma ago, along with the related dramatic deepening of the Nile River Gorge near Luxor, Egypt, could have created the conditions for the gravitational collapse of the eastern escarpment of the Theban Plateau[70].

Ice retreat and deglaciation, accompanied by a whole range of paraglacial effects[129], are a specific set of geo-crises that cause the landscape to become highly prone to landslides for a relatively short transitional period. Numerous landslides in the Patagonian tablelands, especially catastrophic rock avalanches and earthflows, postdate the deglaciation period and could have been triggered by intensified glacioisostatically induced seismic activity at the end of the Pleistocene[34,36,130]. Most landslides in Iceland occurred following deglaciation between 13 ka and 5 ka, during the period of greatest postglacial rebound effects[51,56,57,89,131]. A similar scenario is suggested for rock avalanches in the Vaigat Strait in Greenland, which originated after the retreat of ice sheet at the beginning of the Holocene[38,132].

However, these geological crises might not merely be a matter of protracted geological history. Ongoing activity of certain landslides on tableland rims can also be triggered by more localized anthropogenic factors or environmental problems. For example, what could be the largest documented active landslide on Earth, covering 150 km² of the eastern escarpment of the Ustyurt Plateau, moving at a rate of up to 6 cm per year, could be due to the long-term drop in the level of Lake Aral induced by human activities since the 1960s[133].

Deglaciation, permafrost degradation, change in precipitation patterns and potentially also sea-level rise might reactivate and/or accelerate landslides in high-latitude tablelands such as Greenland[38], Spitsbergen[134] and Antarctic Peninsula[135,136]. These changes in the cryosphere leading to slope instability are already occurring in West Greenland along the Vaigat Strait, owing to progressive warming and resulting in permafrost degradation. This region has had three rock avalanches and frozen debris avalanches since the 1950s, two of them tsunamigenic, with volumes of the order of tens of millions of cubic metres, with source areas in large talus slopes below the caprock basalt[18,137,138] (Box 1).

In summary, although landslides have numerous triggers, the location of tablelands outside major tectonic and seismic zones suggests that most landslides here are due to climatic and/or hydrological triggers. These can be directly related to increased precipitation or climatically driven events (such as changes in ocean levels or deglaciation) that have temporarily altered landscape conditions and promoted slope instability.

Tableland failure over geological time

In the long term, failed tablelands evolve mostly retrogressively, with the activity shifting from the base of the escarpment towards the upper edge. The rotational sliding process is self-stabilizing, as lower displaced blocks form a buttress that redirects (and sometimes inhibits) mass movement activity to higher parts of the slope[12,17,70]. Authors working in the Colorado Plateau[14,32,72] and NW Scotland[121] have observed that as the distance of landslide blocks from the scarp increases, their morphological prominence and roughness decrease, indicating more advanced erosion and greater age. A comparable downslope reduction in the morphological prominence of landslide blocks has been documented in landslides originating in the central Sahara[12], the Nile Valley in Egypt[70] and eastern Patagonia[37]. Changes in surface roughness could be used in the future to date landslide fringes and their reactivations in tablelands, as has already been done for landslides in glacial sediments[139,140] and fold-and-thrust belts[141].

Landslide retrogression causes slope retreat[94] and the consumption of plateaus until complete degradation[6,13,14,41] (Fig. 5). Rotational sliding and spreading are largely gradual, slow processes that result mostly in minute changes in hillslope morphology over individual years; however, occasional catastrophic rock avalanches can cause the escarpment to retreat hundreds of metres instantaneously[91]. Currently, there are limited chronological and monitoring data, but in eastern Patagonia north of Lago Colhué Huapi, for instance, nearly complete plateau consumption with dimensions of 20 km × 5 km occurred in less than 3.5 million years[142], whereas in other regions, only marginal slope retreat has taken place over much longer periods[142]. The final stages of tableland degradation by landslides are marked in the landscape by the occurrence of hummocky slopes and the absence of plateaus or the existence of their remnants only (Fig. 5). In eastern Patagonia, this topography is referred to as 'slumping hummocky landscapes', in places covering hundreds of square kilometres of a former tableland[143].

Some landslide fringes could have formed suddenly without retrogression, and subsequent landslide reactivations took place within the collapsed masses. For example, along the northwest coast of Malta, landslides originated as a first-time failure about 21 ka during the LGM ocean lowstand under a locally wetter climate, but in no connection with coastal erosion[44,95]. Younger movements were then reactivated in the landslide body owing to sea-level rise in the Holocene, caused by the undercutting of the slope through abrasion and saturation of the Blue Clays[95]. Similar landslides, although evolving over a substantially longer period since at least the Early Pleistocene[21,76], are reported from the Black Sea coast of Bulgaria. The currently active parts of these slides are within the reach of current abrasion, that is, along the base of the landslide bodies[21]. The mentioned downslope-advancing landslide events[144] are rather exceptional and limited to specific stretches of landslide fringes, such as zones where landslide toes are repeatedly inundated by water[36,130] and/or oversteepened escarpment sections, subjected to elevated shear stress owing to river or glacial erosion[36], wave action[8], tectonic movements[36] and anthropogenic activity[17,125].

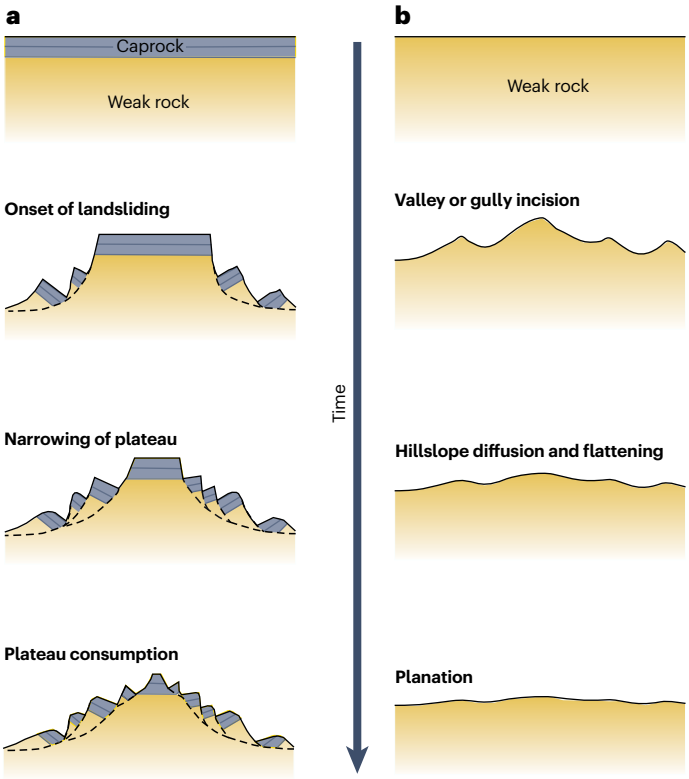

Fig. 5 | Landscape evolution of tablelands with a caprock versus flat plateaus made only of weak rock. a, In a tableland, the protective function of the competent caprock enables the emergence of weak layers in a highly exposed position, making it susceptible to landsliding. Additionally, the caprock on top of rotated blocks facilitates long-term preservation of landslide hummocky morphology. **b**, Without the presence of caprock, fast erosion and terrain flattening will prevail in the weak rocks, resulting in the development of low-gradient hillslopes that inhibit the evolution of landslides.

The tabular structure consisting of caprock overlying mechanically weak beds is responsible for two important aspects of the long-term evolution of landslide fringes (Fig. 5). First, owing to the protective function of the caprock, weak rocks can become exposed on steep, high escarpments that far exceed their critical angle of stability. Without caprock, these weak sediments would quickly be shaped by erosion and diffusive hillslope processes[145,146], limiting the formation of steep, long and high slopes prone to large landslides (Fig. 5). Second, caprock shields detached blocks, enabling their survival in favourable climatic conditions for hundreds of thousands to millions of years[12,70,112,124].

Summary and future perspectives

Landslides around tablelands are controlled by the presence of weak layers and tend to create continuous, topographically largely unconstrained fringes, representing some of the most extensive areas of subaerial slope instability. Determining whether landslide fringes in tablelands are the most extensive is challenging owing to the formation of coalescent landslide areas also in mountainous regions[2], volcanoes[23], volcanic islands[147] and areas with unconsolidated sediments[148].

However, landslide fringes around tableland rims seem to be the most continuous. Compact belts of landslides are less common in

mountains[149] than along the edges of tablelands. Even in mountain ranges composed of extremely landslide-prone rocks (such as flysch, formed by alternating sandstones with unstable claystone beds[150]), we are not aware of landslide fringes that are tens of kilometres long or more. In certain regions such as the Patagonian Andes, volcanic rocks form landslide-fringed tablelands on the foothills of mountains[6], but these fringes are gradually interrupted moving towards the orogenic belt where similar volcanic rocks become tectonically deformed, and increasing tectonic complexity prevents the formation of large coalescent landslide areas (see also Fig. 1). Although giant catastrophic landslides such as rock avalanches occur in these tectonically deformed rocks[34,92,93,151,152], they seldom create continuous fringes. Landslides in sensitive glaciomarine clays (the so-called quick clays) in Canada or Scandinavia are large and numerous but usually lack continuity and cover a maximum area of tens of square kilometres (refs. 153,154). The same applies to other unconsolidated, partially eroded basin fills[148]. In any case, quantifying the area of these various extensive landslide provinces will be essential in the future.

Although the understanding of landslide fringe dynamics and timelines remains limited, it is evident that these landform complexes emerge from the coalescence of numerous individual landslides over time and space, occasionally in conjunction with larger catastrophic events. Although landslide fringes are a typical geomorphological feature along tableland rims, they do not occur in all of the major tablelands of the Earth (Fig. 2). This observation highlights the importance of the geological structure and stratigraphy of escarpments, especially the presence of weak layers below the caprock, in the formation of landslide fringes. Nevertheless, geographical bias in the distribution of failed tablelands is also due to the fragmented knowledge regarding the actual extent and distribution of large landslide fringes. Most known failed tablelands are located in arid regions, easily mapped through optical satellite imagery, but these methods likely lead to underestimations of their presence in forested areas. With increased availability of high-resolution light detection and ranging data in the near future, the picture of an actual distribution of failed tablelands in forested temperate and tropical regions should be a priority of future research. Particular regions to target where extensive landslide fringes are likely to occur could include forested tablelands formed by Mesozoic and Cenozoic sediments east of the Canadian Cordilleras, in tropical areas of Brazil and Africa, in regions with basalt flows in Siberia and in arid platform areas of the Arabian Peninsula, Somalia and yet-to-be-described locations in the Sahara.

Large areas underlain by flat-lying sedimentary and volcanic rock series, with minimal changes in stratigraphy and hence, escarpment morphometry, have resulted in exceptionally long outcrops of weak rocks that cause slope failures spanning hundreds of kilometres along tableland rims (Fig. 1). Because of the protective function of the caprock, mechanically weak rocks can become exposed on steep, high escarpments. However, information on the material properties of these weak layers, responsible for extensive landslide areas moving on very low slopes, often less than 5°, remains sparse[107]. This data gap contrasts with giant submarine landslides, where weak layers have undergone systematic review and categorization[155]. Although flat-lying layered rocks are also present within fold-and-thrust belts and can host landslides (such as the Apennines[156]), the landslide-prone areas constitute relatively small portions of orogenic belts. In any case, elucidating the extreme instability of some of the sedimentary and volcanoclastic rocks forming the sub-caprock layers will require laboratory geomechanical analyses, which have so far only been published for a few tablelands[17].

Caution is needed when interpreting landslide fringes as old and inactive owing to insufficiently long history of observation. Although retrogressive rotational landslides and spreads in arid tablelands can endure for over a million years, remote sensing observations suggest that some of these are still active[42,133]. However, limited information on current movements hinders globally relevant conclusions. Even in arid tablelands with presumed fossil fringes, annual movements ranging from millimetres to centimetres, with occasional faster landslide activity, have been observed since the end of the last millennium[17,19,40,104]. The current morphological footprint of these landslide fringes likely resulted both from cumulative minor events and from major slope failures in short, climatically favourable periods. However, verifying the number of active landslide fringes will only be possible when the database of radiometrically dated and monitored landslides is substantially expanded.

Landslide activity in some tablelands coincides with geological crises. With the impacts of anthropogenic climatic change in mind, the risk of increasing landslide activity in tablelands should be examined further. We anticipate a higher incidence of catastrophic landslides from tablelands in cold regions in the context of climate change, as already observed, notably in West Greenland (Box 1). Furthermore, some subtropical and relatively dry tablelands in South America, Mexico, Africa or the Middle East could be more frequently affected by catastrophic slope processes in the future owing to more frequent extreme rainfall events[157]. In these areas, long-runout landslides, which can result in the damming of valley floors[15,88,127], or landslide tsunamis[38,138], can additionally trigger a chain of various hazards, including flooding, avulsions or outburst floods. It is not excluded that, within the context of climate change, the magnitude of catastrophic landslides could increase beyond what is known from the historical records from these respective regions[17,71].

We summarize that a broader and more complete global inventory of failed tablelands is urgently needed to better understand landslide fringe mechanisms and dynamics. This database can be built through increased global light detection and ranging coverage[158], interferometric synthetic aperture radar-based monitoring[159] and more extensive radiometric dating of landslides[160], enabling more quantified understanding of landslide lifespans and activity across diverse morpho-climatic zones. A more complete picture of past activity, especially during different climate states in the geological past, would improve estimations of the hazards landslide fringes could pose in the context of human-induced climate change.

Published online: 17 September 2024

References

1. Hungr, O., Leroueil, S. & Picarelli, L. The Varnes classification of landslide types, an update. *Landslides* **11**, 167–194 (2014).
2. Korup, O. et al. Giant landslides, topography, and erosion. *Earth Planet. Sci. Lett.* **261**, 578–589 (2007).
3. Hewitt, K., Clague, J. J. & Orwin, J. F. Legacies of catastrophic rock slope failures in mountain landscapes. *Earth Sci. Rev.* **87**, 1–38 (2008).
4. Marc, O. et al. Long-term erosion of the Nepal Himalayas by bedrock landsliding: the role of monsoons, earthquakes and giant landslides. *Earth Surf. Dyn.* **7**, 107–128 (2019).
5. Petley, D. Global patterns of loss of life from landslides. *Geology* **40**, 927–930 (2012).
6. Schönfeldt, E., Winocur, D., Pánek, T. & Korup, O. Deep learning reveals one of Earth's largest landslide terrain in Patagonia. *Earth Planet. Sci. Lett.* **593**, 117642 (2022).
7. Migoń, P. & Duszyński, F. Landscapes and landforms in coarse clastic sedimentary tablelands — is there a unifying theme? *CATENA* **218**, 106545 (2022).
8. Pánek, T., Korup, O., Minár, J. & Hradecký, J. Giant landslides and highstands of the Caspian Sea. *Geology* **44**, 939–942 (2016).
9. Mazzoni, E. & Rabassa, J. Types and internal hydro-geomorphologic variability of mallines (wet-meadows) of Patagonia: emphasis on volcanic plateaus. *J. South Am. Earth Sci.* **46**, 170–182 (2013).

10. Mazzoni, E. & Rabassa, J. Introduction: Patagonia basalt tablelands ('Escoriales') and their significance in the genesis of wetlands. in *Volcanic Landscapes and Associated Wetlands of Lowland Patagonia* (eds Mazzoni, E. & Rabassa, J.) 1–29 (Springer International Publishing, 2018).
11. Nahlik, A. M. & Fennessy, M. S. Carbon storage in US wetlands. *Nat. Commun.* **7**, 13835 (2016).
12. Busche, D. Early quaternary landslides of the Sahara and their significance for geomorphic and climatic history. *J. Arid Environ.* **49**, 429–448 (2001).
13. Strahler, A. N. Landslides of the Vermilion and Echo cliffs, northern Arizona. *J. Geomorphol.* **3**, 285–301 (1940).
14. Ahnert, F. The influence of Pleistocene climates upon the morphology of cuesta scarps on the Colorado Plateau. *Ann. Assoc. Am. Geograph.* **50**, 139–156 (1960).
15. Reneau, S. L. & Dethier, D. P. Late Pleistocene landslide-dammed lakes along the Rio Grande, White Rock Canyon, New Mexico. *GSA Bull.* **108**, 1492–1507 (1996).
16. Coe, J. A. et al. Rock-avalanche dynamics revealed by large-scale field mapping and seismic signals at a highly mobile avalanche in the West Salt Creek valley, western Colorado. *Geosphere* **12**, 607–631 (2016).
17. Watkins, C. M. & Rogers, J. D. A new look at landslides of the Vermilion and Echo Cliffs, Northern Arizona. *Environ. Eng. Geosci.* **28**, 173–192 (2022).
18. Svennevig, K. et al. A large frozen debris avalanche entraining warming permafrost ground — the June 2021 Assapaat landslide, West Greenland. *Landslides* **19**, 2549–2567 (2022).
19. Schoeneich, P. & Bouzou, I. Landslides in Niger (Western Africa). in *Lanslides. Glissements de terrain* (ed. Kaare, S.) 1967–1972 (Balkema, 1996).
20. Sæmundsson, Th., Pétursson, H. G., Kneisel, C. & Beylich, A. A. Monitoring of the Tjarnardalir landslide, in central North Iceland. *First North Am. Landslide Conf.* **23**, 1029–1040 (2007).
21. Evstatiev, D. & Evlogiev, Y. Landslides along the northern Black Sea coast between Varna city and Kavarna town (Bulgaria). *Geo-Eco-Marina* **19/2013**, 39–57 (2013).
22. Mantovani, M., Devoto, S. & Forte, E. A multidisciplinary approach for rock spreading and block sliding investigation in the north-western coast of Malta. *Landslides* **10**, 611–622 (2013).
23. Dufresne, A., Siebert, L. & Bernard, B. Distribution and geometric parameters of volcanic debris avalanche deposits. in *Volcanic Debris Avalanches* (eds Roverato, M., Dufresne, A. & Proter, J.) 75–90 (Springer, 2021).
24. Zhuang, J. et al. Distribution and characteristics of landslide in Loess Plateau: a case study in Shaanxi province. *Eng. Geol.* **236**, 89–96 (2018).
25. Kong, J. et al. Failure mechanism and movement process of three loess landslides due to freeze–thaw cycle in the Fangtai village, Yongjing County, Chinese Loess Plateau. *Eng. Geol.* **315**, 107030 (2023).
26. Bjerrum, L. Stability of natural slopes in quick clay. *Géotechnique* **5**, 101–119 (1955).
27. Bryn, P., Berg, K., Forsberg, C. F., Solheim, A. & Kvalstad, T. J. Explaining the Storegga Slide. *Mar. Petrol. Geol.* **22**, 11–19 (2005).
28. Vanneste, M., Mienert, J. & Bünz, S. The Hinlopen Slide: a giant, submarine slope failure on the northern Svalbard margin, Arctic Ocean. *Earth Planet. Sci. Lett.* **245**, 373–388 (2006).
29. Elger, J. et al. Chronology of the fram slide complex offshore NW Svalbard and its implications for local and regional slope stability. *Mar. Geol.* **393**, 141–155 (2017).
30. Brunetti, M. T. et al. Analysis of a new geomorphological inventory of landslides in Valles Marineris, Mars. *Earth Planet. Sci. Lett.* **405**, 156–168 (2014).
31. Crosta, G. B., Frattini, P., Valbuzzi, E. & De Blasio, F. V. Introducing a new inventory of large Martian landslides. *Earth Space Sci.* **5**, 89–119 (2018).
32. Reiche, P. The Toreva-block — a distinctive landslide type. *J. Geol.* **45**, 538–548 (1937).
33. Robertson, J. E., Karlstrom, K. E., Heizler, M. T. & Crossey, L. J. Realignments of the Colorado River by ~2 m.y. of rotational bedrock landsliding: the Surprise Valley landslide complex, Grand Canyon, Arizona. *Geosphere* **17**, 1715–1744 (2021).
34. Pánek, T., Korup, O., Lenart, J., Hradecký, J. & Březný, M. Giant landslides in the foreland of the Patagonian Ice Sheet. *Quater. Sci. Rev.* **194**, 39–54 (2018).
35. Pánek, T., Březný, M., Harrison, S., Schönfeldt, E. & Winocur, D. Large landslides cluster at the margin of a deglaciated mountain belt. *Sci. Rep.* **12**, 5658 (2022).
36. Pánek, T. et al. The largest rock avalanches in Patagonia: timing and relation to Patagonian Ice Sheet retreat. *Quater. Sci. Rev.* **302**, 107962 (2023).
37. Schönfeldt, E., Pánek, T., Winocur, D., Šilhán, K. & Korup, O. Postglacial Patagonian mass movement: from rotational slides and spreads to earthflows. *Geomorphology* **367**, 107316 (2020).
38. Svennevig, K. et al. Holocene gigascale rock avalanches in Vaigat strait, West Greenland — implications for geohazard. *Geology* **52**, 147–152 (2024).
39. Svennevig, K. Preliminary landslide mapping in Greenland. *GEUS Bull.* **43**, 5 (2019).
40. Schoeneich, P. & Bouzou, I. Glissements de terrain dans l'Adar (Niger). in *Geowissenschaftliche Untersuchungen in Afrika* Vol. 69 (eds Hagedorn, H. & Baumhauer, R.) 149–165 (Würzburg, 1988).
41. Mège, D., Le Deit, L., Rango, T. & Korme, T. Gravity tectonics of topographic ridges: halokinesis and gravitational spreading in the western Ogaden, Ethiopia. *Geomorphology* **193**, 1–13 (2013).
42. Aslan, G., De Michele, M., Raucoules, D., Bernardie, S. & Cakir, Z. Transient motion of the largest landslide on earth, modulated by hydrological forces. *Sci. Rep.* **11**, 10407 (2021).
43. Mège, D. et al. Large-scale gravitational spreading in Southeast Ethiopia. in *Geomorphology for Human Adaptation to Changing Tropical Environments* (eds Asrat, A. & Dramis, F.) (Addis Ababa, 2011).
44. Foglini, F. et al. Late Quaternary coastal landscape morphology and evolution of the Maltese Islands (Mediterranean Sea) reconstructed from high resolution seafloor data. in *Geology and Archaeology: Submerged Landscapes of the Continental Shelf* Vol. 411 (eds Harff, J., Bailey, G. & Lüth, F.) 77–95 (Geological Society, 2015).
45. Prampolini, M. et al. Geomorphological mapping of terrestrial and marine areas, northern Malta and Comino (central Mediterranean Sea). *J. Maps* **13**, 457–469 (2017).
46. Moeyersons, J. et al. Mass movement mapping for geomorphological understanding and sustainable development: Tigray, Ethiopia. *CATENA* **75**, 45–54 (2008).
47. Van Den Eeckhaut, M. et al. Spatial patterns of old, deep-seated landslides: a case-study in the northern Ethiopian highlands. *Geomorphology* **105**, 239–252 (2009).
48. Kropáček, J., Vařilová, Z. & Nyssen, J. Historical aerial and terrestrial photographs for the investigation of mass movement dynamics in the Ethiopian Highlands. *Land Degrad. Dev.* **30**, 483–493 (2019).
49. Nyssen, J., Moeyersons, J., Poesen, J., Deckers, J. & Mitiku, H. The environmental significance of the remobilisation of ancient mass movements in the Atbara–Tekeze headwaters, Northern Ethiopia. *Geomorphology* **49**, 303–322 (2003).
50. Whalley, W. B., Douglas, G. R. & Jonsson, A. The magnitude and frequency of large rockslides in Iceland in the postglacial. *Geografiska Annaler. Ser. A Phys. Geogr.* **65**, 99–110 (1983).
51. Cossart, E. et al. Impacts of post-glacial rebound on landslide spatial distribution at a regional scale in northern Iceland (Skagafjörður). *Earth Surf. Process. Landf.* **39**, 336–350 (2014).
52. Feuillet, T. et al. Focusing on the spatial non-stationarity of landslide predisposing factors in northern Iceland: do paraglacial factors vary over space? *Prog. Phys. Geogr.* **38**, 354–377 (2014).
53. Decaulne, A. et al. An early Holocene age for the Vatn landslide (Skagafjörður, central northern Iceland): insights into the role of postglacial landsliding on slope development. *Holocene* **26**, 1304–1318 (2016).
54. Peras, A., Decaulne, A., Cossart, E., Coquin, J. & Mercier, D. Distribution and spatial analysis of rockslides failures in the Icelandic Westfjords: first results. *Géomorphologie* **22**, 25–35 (2016).
55. Portier, E., Mercier, D. & Decaulne, A. Spatial analysis and controlling factors of landslides in East Icelandic fjords. *Géomorphologie* **29**, 17634 (2023).
56. Coquin, J., Mercier, D., Bourgeois, O., Cossart, E. & Decaulne, A. Gravitational spreading of mountain ridges coeval with Late Weichselian deglaciation: impact on glacial landscapes in Tröllaskagi, northern Iceland. *Quater. Sci. Rev.* **107**, 197–213 (2015).
57. Coquin, J., Mercier, D., Bourgeois, O., Feuillet, T. & Decaulne, A. Is gravitational spreading a precursor for the Stífluhólar landslide (Skagafjörður, Northern Iceland)? *Géomorphologie* **22**, 9–24 (2016).
58. Rybář, J., Stemberk, J. & Hartvich, F. Slope failures around the rock castle Drábské světničky, Czech Republic. *Acta Geodyn. Geomater.* **4**, 51–65 (2006).
59. Duszyński, F., Jancewicz, K., Kasprzak, M. & Migoń, P. The role of landslides in downslope transport of caprock-derived boulders in sedimentary tablelands, Stołowe Mts, SW Poland. *Geomorphology* **295**, 84–101 (2017).
60. Stemberk, J., Hartvich, F., Blahůt, J., Rybář, J. & Krejčí, O. Tectonic strain changes affecting the development of deep seated gravitational slope deformations in the Bohemian Massif and Outer Western Carpathians. *Geomorphology* **289**, 3–17 (2017).
61. Schmidt, K. H. & Beyer, I. Factors controlling mass movement susceptibility on the Wellenkalk-scarp in Hesse and Thuringia. *Z. fur Geomorphologie, Supplementband* **125**, 43–63 (2001).
62. Schmidt, K.-H. & Beyer, I. High-magnitude landslide events on a limestone-scarp in central Germany: morphometric characteristics and climatic controls. *Geomorphology* **49**, 323–342 (2003).
63. Yenes, M., Monterrubio, S., Nespereira, J. & Santos, G. Geometry and kinematics of a landslide surface in tertiary clays from the Duero Basin (Spain). *Eng. Geol.* **104**, 41–54 (2009).
64. Yenes, M., Monterrubio, S., Nespereira, J., Santos, G. & Fernández-Macarro, B. Large landslides induced by fluvial incision in the Cenozoic Duero Basin (Spain). *Geomorphology* **246**, 263–276 (2015).
65. Knight, J. Deglaciation and paraglacial landsliding in the Antrim Glens: an example from Garron Point. in *North of Ireland: Field Guide* (eds Whitehouse, N. J., Roe, H. M., McCarron, S. & Knight, J.) 129–136 (Quaternary Research Association, 2008).
66. Southall, D. W. et al. Age evaluation and causation of rock-slope failures along the western margin of the Antrim Lava Group (ALG), Northern Ireland, based on cosmogenic isotope (36Cl) surface exposure dating. *Geomorphology* **285**, 235–246 (2017).
67. Stengel, I. Fossil landslides in the Schwarzrand, Huib and Huns escarpment areas — a contribution to the quaternary morphostratigraphy of Southern Namibia. *Paleoecol. Afr. Surround. Isl.* **27**, 221–238 (2001).
68. Slee, A. et al. The age and paleoclimate implications of relict periglacial block deposits on the New England Tablelands, Australia. *Quater. Res.* **111**, 121–137 (2023).
69. Selby, M. J. *Hillslope Materials and Processes* (Oxford Univ. Press, 1993).
70. Dupuis, C. et al. Genesis and geometry of tilted blocks in the Theban Hills, near Luxor (Upper Egypt). *J. Afr. Earth Sci.* **61**, 245–267 (2011).
71. Peulvast, J.-P., Bétard, F. & de Oliveira Magalhães, A. Scarp morphology and identification of large-scale mass movements in tropical tablelands: the eastern Araripe basin (Ceará, Brazil). *Géomorphologie* **17**, 33–52 (2011).
72. Baum, R. L. & Odum, J. K. *Geologic Map of Slump-Block Deposits in Part of the Grand Mesa Area, Delta and Mesa Counties* Vol. 1 (United States Geological Survey, 1996).
73. Gerath, R. F. & Hungr, O. Active earth: landslide terrain, Scatter River Valley, Northeastern British Columbia. *Geosci. Canada* **10**, 30–32 (1983).

74. Fenton, C., Martin, P., Cheng, F. & Murphy, B. Geomorphological analysis of large scale slope instability, Trotternish, Isle of Skye. *Eng. Geol. Soc. Territory* **2**, 1037–1040 (2015).
75. Devoto, S. et al. Geomorphological map of the NW coast of the island of Malta, Mediterranean Sea.*J. Maps* **8**, 33–40 (2012).
76. Evstatiev, D. & Evlogiev, Y. On the origin of the 'Ikantalaka' landslide — the Balchik coast. *Geol. Balcanica* **36**, 25–30 (2007).
77. Berov, B., Ivanov, P., Dobrev, N., Nankin, R. & Krastanov, M. *State of the Art for Landslides Along the North Bulgarian Black Sea Coast* 97–112 (Springer, 2013).
78. Watson, R. A. & Wright, H. E. Landslides on the east flank of the Chuska Mountains, northwestern New Mexico. *Am. J. Sci.* **261**, 525–548 (1963).
79. Grunert, J. Geomorphologie der Schichtstufen am Westrand des Murzuk-Beckens (Zentrale Sahara).*Relief-Boden-Palaöklima* **2**, 271 (1983).
80. Pasuto, A., Soldati, M. & Tecca, P. R. 5.10 — lateral spread: from rock to soil spreading. in *Treatise on Geomorphology* 2nd edn (ed. Shroder, J.) 169–182 (Academic Press, 2022).
81. Moore, J. M. & Schultz, R. A. Processes of faulting in jointed rocks of Canyonlands National Park, Utah. *Geol. Soc. Am. Bull.* **111**, 808–822 (1999).
82. Gutiérrez, F. Origin of the salt valleys in the Canyonlands section of the Colorado Plateau: evaporite-dissolution collapse versus tectonic subsidence. *Geomorphology* **57**, 423–435 (2004).
83. Schultz-Ela, D. D. & Walsh, P. Modeling of grabens extending above evaporites in Canyonlands National Park. *Utah J. Struct. Geol.* **24**, 247–275 (2002).
84. Goldscheider, N., Chen, Z. & Auler, A. S. Global distribution of carbonate rocks and karst water resources. *Hydrogeol. J.* **28**, 1661–1677 (2020).
85. Davies, T. R., McSaveney, M. J. & Hodgson, K. A. A fragmentation-spreading model for long-runout rock avalanches. *Can. Geotech. J.* **36**, 1096–1110 (1999).
86. Aaron, J. & McDougall, S. Rock avalanche mobility: the role of path material. *Eng. Geol.* **257**, 105126 (2019).
87. Safran, E. B., Anderson, S. W., Mills-Novoa, M., House, P. K. & Ely, L. Controls on large landslide distribution and implications for the geomorphic evolution of the southern interior Columbia River basin. *Geol. Soc. Am. Bull.* **123**, 1851–1862 (2011).
88. Safran, E. B. et al. Plugs or flood-markers? The unstable landslide dams of eastern Oregon. *Geomorphology* **248**, 237–251 (2015).
89. Mercier, D. et al. The Höfðahólar rock avalanche (Sturzström): chronological constraint of paraglacial landsliding on an Icelandic hillslope. *Holocene* **23**, 432–446 (2013).
90. White, J. L., Morgan, M. L. & Berry, K. A. The West Salt Creek landslide: a catastrophic rockslide and rock/debris avalanche in Mesa County, Colorado. *Colo. Geol. Surv. Bull.* **55**, 2 (2015).
91. Peulvast, J. P. & Bétard, F. A history of basin inversion, scarp retreat and shallow denudation: the Araripe basin as a keystone for understanding long-term landscape evolution in NE Brazil. *Geomorphology* **233**, 20–40 (2015).
92. Penna, I. M., Hermanns, R. L., Niedermann, S. & Folguera, A. Multiple slope failures associated with neotectonic activity in the Southern Central Andes (37°–37°30'S), Patagonia, Argentina. *GSA Bull.* **123**, 1880–1895 (2011).
93. Penna, I. M., Hermanns, R. L., Daicz, S., Suriano, J. & Tedesco, A. M. Effects of tectonic deformation and landslides in the erosion of a mountain plateau in the transitional zone between the central and Patagonian Andes. *Am. J. Sci.* **315**, 257–274 (2015).
94. Duszyński, F., Migoń, P. & Strzelecki, M. C. Escarpment retreat in sedimentary tablelands and cuesta landscapes — landforms, mechanisms and patterns. *Earth Sci. Rev.* **196**, 102890 (2019).
95. Soldati, M., Barrows, T. T. & Prampolini, M. Cosmogenic exposure dating constraints for coastal landslide evolution on the Island of Malta (Mediterranean Sea).*J. Coast. Conserv.* **22**, 831–844 (2018).
96. Flint, R. F. & Denny, C. S. Quaternary geology of Boulder Mountain Aquarius Plateau, Utah. *Geol. Surv. Bull.* **1061-D**, 103–164 (1958).
97. Marchetti, D. W., Cerling, T. E., Dohrenwend, J. C. & Gallin, W. Ages and significance of glacial and mass movement deposits on the west side of Boulder Mountain, Utah, USA. *Palaeogeogr. Palaeoclimatol. Palaeoecol.* **252**, 503–513 (2007).
98. Krijgsman, W. et al. Quaternary time scales for the Pontocaspian domain: interbasinal connectivity and faunal evolution. *Earth Sci. Rev.* **188**, 1–40 (2019).
99. Aubrecht, R. et al. Sandstone caves on Venezuelan tepuis: return to pseudokarst? *Geomorphology* **132**, 351–365 (2011).
100. Hamza, O., De Vargas, T., Boff, F. E., Hussain, Y. & Sian Davies-Vollum, K. Geohazard assessment of landslides in South Brazil: case Study. *Geotech. Geol. Eng.* **38**, 971–984 (2020).
101. Joshi, M. et al. Weathering controlled landslide in Deccan traps: insight from Mahabaleshwar, Maharashtra. *J. Geol. Soc. India* **92**, 555–561 (2018).
102. Singh, R. G., Botha, G. A., Richards, N. P. & McCarthy, T. S. Holocene landslides in KwaZulu-Natal, South Africa. *South Afr. J. Geol.* **111**, 39–52 (2008).
103. Kycl, P. et al. Tectonic control of complex slope failures in the Ameka River Valley (Lower Gibe Area, central Ethiopia): implications for landslide formation. *Geomorphology* **288**, 175–187 (2017).
104. Ostaficzuk, S. Large-scale landslides in North-Western Libya. *Acta Geol. Pol.* **23**, 231–244 (1973).
105. Mantovani, M. et al. Coupling long-term GNSS monitoring and numerical modelling of lateral spreading for hazard assessment purposes. *Eng. Geol.* **296**, 106466 (2022).
106. Pánek, T. et al. A megalandslide in the Northern Caucasus foredeep (Uspenskoye, Russia): geomorphology, possible mechanism and age constraints. *Geomorphology* **177–178**, 144–157 (2012).
107. Xin, P., Liu, Z., Wu, S., Liang, C. & Lin, C. Rotational–translational landslides in the neogene basins at the northeast margin of the Tibetan Plateau. *Eng. Geol.* **244**, 107–115 (2018).
108. Davidson, E. S. *Geology of the Circle Cliffs Area, Garfield and Kane Counties, Utah. Bulletin*. https://pubs.usgs.gov/publication/b1229 (1967).
109. Břežný, M. & Pánek, T. Deep-seated landslides affecting monoclinal flysch morphostructure: evaluation of LiDAR-derived topography of the highest range of the Czech Carpathians. *Geomorphology* **285**, 44–57 (2017).
110. Fan, Y., Toran, L. & Schlische, R. W. Groundwater flow and groundwater-stream interaction in fractured and dipping sedimentary rocks: insights from numerical models. *Water Res. Res.* https://doi.org/10.1029/2006WR004864 (2007).
111. Klimeš, J. et al. The monitoring of slow-moving landslides and assessment of stabilization measures using an optical-mechanical crack gauge. *Landslides* **9**, 407–415 (2012).
112. Grunert, J. & Busche, D. Large scale fossil landslides at the Msāk Mallat and Hamādat Mānghīnī Escarpment. in *The Geology of Libya* Vol. III (eds Salem, M. J. & Busrewil, M. R.) 849–860 (Academic Press, 1980).
113. Dethier, D. P. & Reneau, S. L. Lacustrine chronology links Late Pleistocene climate change and mass movements in northern New Mexico. *Geology* **24**, 539–542 (1996).
114. Fleitmann, D. et al. Holocene and Pleistocene pluvial periods in Yemen, southern Arabia. *Quater. Sci. Rev.* **30**, 783–787 (2011).
115. Nicholson, S. L. Pluvial periods in Southern Arabia over the last 1.1 million-years. *Quater. Sci. Rev.* **229**, 106112 (2020).
116. Skonieczny, C., Paillou, P. & Bory, A. African humid periods triggered the reactivation of a large river system in Western Sahara. *Nat. Commun.* **6**, 8751 (2015).
117. Blanchet, C. L., Osborne, A. H. & Tjallingii, R. Drivers of river reactivation in North Africa during the last glacial cycle. *Nat. Geosci.* **14**, 97–103 (2021).
118. Ballantyne, C. K., Stone, J. O. & Fifield, L. K. Cosmogenic Cl-36 dating of postglacial landsliding at the Storr, Isle of Skye, Scotland. *Holocene* **8**, 347–351 (1998).
119. Shurtliff, R. Wetlands on the thousand lake mountain mega-landslide as paleoclimate proxies. *Theses and Dissertations* (2014).
120. Shurtliff, R. A. et al. A 13000 year multi-proxy climate record from central Utah (western USA), emphasizing conditions leading to large mass movements. *Boreas* **46**, 308–324 (2017).
121. Ballantyne, C. K. Scottish landforms examples 2, The landslides of Trotternish, Isle of Skye. *Scott. Geogr. Mag.* **107**, 130–135 (1991).
122. Ramos, V. A., Niemeyer, H., Skarmeta, J. & Mun˜oz, J. Magmatic evolution of the Austral Patagonian Andes. *Earth Sci. Rev.* **18**, 411–443 (1982).
123. Cobos, J. C., Anselmi, G., Panza, J. L. A., Giacosa, R. E. & Escosteguy, L. D. *Hoja Geológica 4972-IV Tres Lagos* (Servicio Geológico Minero Argentino, Instituto de Geología y Recursos Minerales, 2009).
124. Bardají, T. et al. Geomorphology of Dra Abu el-Naga (Egypt): the basis of the funerary sacred landscape. *J. Afr. Earth Sci.* **131**, 233–250 (2017).
125. McCormick, W. V., Richmond, J. C. & Dahlen, K. *Revised Geotechnical Assessment Bitter Springs Landslide US Highway* 89 *MP* 526 *ER*-089*E*(205)*T Tracs H* 8641 01*D* (2014).
126. Hilger, P. et al. Multiple rock-slope failures from Mannen in Romsdal Valley, western Norway, revealed from Quaternary geological mapping and ^{10}Be exposure dating. *Holocene* **28**, 1841–1854 (2018).
127. Arzhannikova, A. V., Arzhannikov, S. G. & Akulova, V. V. Traces of dammed paleolake activity in the main valley relief and fill in the south of the Irkutsk amphitheater. *Russ. Geol. Geophys.* **49**, 124–131 (2008).
128. Arzhannikov, S. G. et al. Catastrophic events in the quaternary outflow history of Lake Baikal. *Earth Sci. Rev.* **177**, 76–113 (2018).
129. Ballantyne, C. K. Paraglacial geomorphology. *Quaternary Sci. Rev.* **21**, 1935–2017 (2002).
130. Pánek, T. et al. Moraines and marls: giant landslides of the Lago Pueyrredón valley in Patagonia, Argentina. *Quater. Sci. Rev.* **248**, 106598 (2020).
131. Mercier, D. et al. Are Icelandic rock-slope failures paraglacial? Age evaluation of seventeen rock-slope failures in the Skagafjörður area, based on geomorphological stacking, radiocarbon dating and tephrochronology. *Geomorphology* **296**, 45–58 (2017).
132. Korsgaard, N. J. et al. Evidence of middle Holocene landslide-generated tsunamis recorded in lake sediments from Saqqaq, West Greenland. *Nat. Hazards Earth Syst. Sci.* **24**, 757–772 (2024).
133. Aslan, G. et al. Dynamics of a giant slow landslide complex along the coast of the Aral Sea, Central Asia. *Turkish J. Earth Sci.* **32**, 819–832 (2023).
134. Kuhn, D. et al. Anatomy of a mega-rock slide at Forkastningsfjellet, Spitsbergen and its implications for landslide hazard and risk considerations. *Nor. J. Geol.* **99**, 41–61 (2019).
135. Davies, B. J. et al. Landscape evolution and ice-sheet behaviour in a semi-arid polar environment: James Ross Island, NE Antarctic Peninsula. *Geol. Soc. Lond. Spec. Publ.* **381**, 353–395 (2013).
136. Jennings, S. J. A. et al. Geomorphology of Ulu Peninsula, James Ross Island, Antarctica. *J. Maps* **17**, 125–139 (2021).
137. Dahl-Jensen, T. et al. Landslide and tsunami 21 November 2000 in Paatuut, West Greenland. *Nat. Hazards* **31**, 277–287 (2004).
138. Svennevig, K. et al. Uncovering a 70-year-old permafrost degradation induced disaster in the Arctic, the 1952 Niiortuut landslide-tsunami in central West Greenland. *Sci. Total Environ.* **859**, 160110 (2023).
139. LaHusen, S. R., Duvall, A. R., Booth, A. M. & Montgomery, D. R. Surface roughness dating of long-runout landslides near Oso, Washington (USA), reveals persistent postglacial hillslope instability. *Geology* **44**, 111–114 (2016).

140. Booth, A. M., LaHusen, S. R., Duvall, A. R. & Montgomery, D. R. Holocene history of deep-seated landsliding in the North Fork Stillaguamish River valley from surface roughness analysis, radiocarbon dating, and numerical landscape evolution modeling: landsliding in the N. Fork Stillaguamish. *J. Geophys. Res. Earth Surf.* **122**, 456–472 (2017).
141. LaHusen, S. R. et al. Rainfall triggers more deep-seated landslides than Cascadia earthquakes in the Oregon Coast Range, USA. *Sci. Adv.* **6**, eaba6790 (2020).
142. Haller, M. J., Massaferro, G. I., Alric, V. I., Navarrete, C. R. & Menegatti, N. Cenozoic intraplate magmatism of central Patagonia, Argentina. *J. South Am. Earth Sci.* **102**, 102650 (2020).
143. Mazzoni, E. & Rabassa, J. An evolutionary model of volcanic landscapes. in *Volcanic Landscapes and Associated Wetlands of Lowland Patagonia. The Latin American Studies Book Series* (eds Mazzoni, E. & Rabassa, J.) 155–176 (Springer, 2018).
144. Cruden, D. M. & Varness, D. J. Landslide types and processes. in *Landslides: Investigation and Mitigation* Vol. 247 (eds Turner, K. A. & Schuster, R. L.) 36–75 (National Academy Press, 1996).
145. Fernandes, N. F. & Dietrich, W. E. Hillslope evolution by diffusive processes: the time scale for equilibrium adjustments. *Water Resour. Res.* **33**, 1307–1318 (1997).
146. Mudd, S. M. & Furbish, D. J. Responses of soil-mantled hillslopes to transient channel incision rates. *J. Geophys. Res. Earth Surface* **112**, JF000516 (2007).
147. Blahůt, J. et al. A comprehensive global database of giant landslides on volcanic islands. *Landslides* **16**, 2045–2052 (2019).
148. Hermanns, R. et al. Relation of recent megalandslides to prehistoric events in the city of La Paz, Bolivia. in *Landslides and Engineered Slopes: Protecting Society Through Improved Understanding* 265–271 (Taylor & Francis, 2012).
149. Crosta, G. B., Frattini, P. & Agliardi, F. Deep seated gravitational slope deformations in the European Alps. *Tectonophysics* **605**, 13–33 (2013).
150. Pánek, T., Břežný, M., Kapustová, V., Lenart, J. & Chalupa, V. Large landslides and deep-seated gravitational slope deformations in the Czech Flysch Carpathians: new LiDAR-based inventory. *Geomorphology* **346**, 106852 (2019).
151. González Díaz, E., Fauque, L., Giaccardi, A. & Costa, C. Las lagunas de varvar co campos y varvar co tapia (N del Neuquén, Argentina): Su relación con avalanchas de rocas. *Rev. de la Asociación Geológica Argentina* **55**, 147–164 (2000).
152. González Díaz, E. F., Folguera, A. & Hermanns, R. La avalancha de rocas del cerro Los Cardos (37°10′ S, 70°53′ O) en la región norte de la provincia del Neuquén. *Rev. de la Asociación Geológica Argentina* **60**, 207–220 (2005).
153. Brooks, G. R. A massive sensitive clay landslide, Quyon Valley, southwestern Quebec, Canada, and evidence for a paleoearthquake triggering mechanism. *Quater. Res.* **80**, 425–434 (2013).
154. Brooks, G. R. & Perret, D. A long-term context for the 1663 Charlevoix CE earthquake interpreted from the postglacial landslide record in the Gouffre Valley, Quebec, Canada. *Quater. Sci. Rev.* **309**, 108096 (2023).
155. Gatter, R., Clare, M. A., Kuhlmann, J. & Huhn, K. Characterisation of weak layers, physical controls on their global distribution and their role in submarine landslide formation. *Earth-Sci. Rev.* **223**, 103845 (2021).
156. Conti, S. & Tosatti, G. Landslides affecting tabular rocks in complex geological situations: the case of Sasso di Simone and Simoncello (Northern Apennines, Italy). In. *Landslides Proc. Seventh ICFL, Czech Slovak. Repub.* **28**, 219–224 (1993).
157. Gariano, S. L. & Guzzetti, F. Landslides in a changing climate. *Earth Sci. Rev.* **162**, 227–252 (2016).
158. Jaboyedoff, M. et al. Use of LIDAR in landslide investigations: a review. *Nat. Hazards* **61**, 5–28 (2012).
159. Casagli, N., Intrieri, E., Tofani, V., Gigli, G. & Raspini, F. Landslide detection, monitoring and prediction with remote-sensing techniques. *Nat. Rev. Earth Environ.* **4**, 51–64 (2023).
160. Pánek, T. Recent progress in landslide dating: a global overview. *Prog. Phys. Geogr. Earth Environ.* **39**, 168–198 (2015).
161. Solle, G. Felsgleitungen in Oberägypten: ein Beitrag zum Ablauf großer Gleitungssysteme. *Notizbl. des. Hessischen Landesamts für Bodenforsch.* **95**, 117–147 (1967).
162. Dam, G. et al. Lithostratigraphy of the Cretaceous–Paleocene Nuussuaq Group, Nuussuaq Basin, West Greenland. *GEUS Bull.* **19**, 1–171 (2009).
163. Pedersen, A. K., Larsen, L. M. & Pedersen, G. K. Lithostratigraphy, geology and geochemistry of the volcanic rocks of the Vaigat Formation on Disko and Nuussuaq. *Paleocene West Greenland GEUS Bull.* **39**, 1–244 (2017).
164. Pedersen, A. K., Larsen, L. M. & Pedersen, G. K. Lithostratigraphy, geology and geochemistry of the volcanic rocks of the Maligât Formation and associated intrusions on Disko and Nuussuaq, Paleocene West Greenland. *GEUS Bull.* **40**, 1–239 (2018).

Acknowledgements
This Review was conducted within the framework of the Czech Science Foundation, project 23-07310S.

Author contributions
T.P. and K.S. researched data for the article. All authors contributed substantially to discussion of the content. T.P. and K.S. wrote the article. All authors reviewed and/or edited the manuscript before submission.

Competing interests
The authors declare no competing interests.

Additional information
Supplementary information The online version contains supplementary material available at https://doi.org/10.1038/s43017-024-00587-1.

Peer review information *Nature Reviews Earth & Environment* thanks R. Hermanns, M. Soldati and the other, anonymous, reviewer(s) for their contribution to the peer review of this work.